The cryptic origins of evolutionary novelty: 1,000-fold-faster trophic diversification rates without increased ecological opportunity or hybrid swarm

CHRISTOPHER H. MARTIN[1]

[1]*Department of Biology, University of North Carolina at Chapel Hill, NC, USA*

Running Title: Ecological opportunity and the origins of novelty

Key words: adaptive radiation, ecological opportunity, innovation, novelty, macroevolution, diversification rate, ecological speciation, trophic divergence

Correspondence: Christopher H Martin. Department of Biology, University of North Carolina at Chapel Hill, Campus Box 3280, 120 South Rd., NC, 27599, USA

Email: chmartin@unc.edu

Data accessibility: All datasets used for this study will be deposited in Dryad. All Illumina reads sequenced will be deposited in the NCBI Short Read Archive.

Table S1-S3, Appendix S1, Figures S1-S4, Supplemental Methods

Table S1. Analysis of shifts in trait diversification rates for 28 skeletal traits measured in Caribbean pupfishes (Fig 1). Median rates on San Salvador Island, Bahamas were estimated for each trait from a multi-rate Brownian motion process using reversible-jump MCMC sampling in *auteur* (Eastman et al. 2011). The background rate was the median rate across all taxa. The posterior probability of a shift to a new diversification rate regime on a San Salvador branch (nearly always the branch leading to the three scale-eater populations) is also shown. The three fastest diversifying traits on San Salvador are highlighted in bold.

	median rate	background rate	relative rate	probably of rate shift on San Salvador
1. Jaw length	**259.5**	**8.43**	**30.8**	**0.49**
2. Dentary length	126.74	9.45	13.4	0.40
3. Jaw opening lever	3.71	2.40	1.55	0.12
4. Jaw closing lever	6.78	4.75	1.43	0.13
5. Coronoid width	**233.35**	**10.30**	**22.7**	**0.68**
6. Angular length	1.79	1.18	1.52	0.19
7. Retroarticular width	69.36	6.25	11.1	0.44
8. Tooth length	1.97	1.08	1.82	0.24
9. Premaxilla width	4.6	3.2	1.44	0.19
10. Premaxilla length	**308.9**	**23.1**	**13.4**	**0.40**
11. Upper jaw length	1.43	0.93	1.54	0.18
12. Premaxilla thickness	5.11	3.19	1.60	0.40
13. Dentigerous process width	11.57	2.46	4.70	0.28
14. Ascending process length	11.10	8.00	1.39	0.20
15. Maxilla length	0.256	0.585	0.44	0.36
16. Maxilla rotating arm	5.78	2.23	2.59	0.18
17. Maxilla thickness	11.36	4.41	2.58	0.14
18. Maxilla head protrusion	4.09	1.47	2.78	0.32
19. Orbit diameter	0.06	0.05	1.20	0.04
20. Neurocranium length	1.2	3.7	0.32	0.04
21. Neurocranium height	1.04	0.72	1.44	0.17
22. Palatine length	12.05	2.68	4.50	0.37
24. Pectoral height	0.45	0.28	1.61	0.27
25. Pectoral length	52.91	18.06	2.93	0.24
26. Adductor mandibulae height	0.82	1.05	0.78	0.08
27. Adductor mandibulae length	57.77	27.20	2.12	0.48
28. Quadrate length	2.00	1.38	1.45	0.24

Table S2. Comparison of dietary/morphological diversity of generalist populations between allopatric and sympatric (including 1 or more pupfish specialist species) lake populations on San Salvador Island (1-way ANOVA). Morphological and stable isotope diversity indices were combined for multiple analysis of variance (MANOVA) and the significance of Pillai's trace (0.721) is presented.

variable	***df***	***P***
Combined	10	0.31
stomach content diversity	6	0.36
δ13C	10	0.67
δ15N	10	0.75
PC1 variance	10	0.13
PC2 variance	10	0.38
LD1 variance	10	0.28
LD2 variance	10	0.10

Table S3. Tests for differential gene flow into San Salvador specialist species using the f_4 statistic calculated in Treemix (Pickrell and Pritchard 2012). Significant f_4 statistics indicate violation of the four-population tree model for that subset of populations, supporting additional gene flow between A ↔ C and/or B ↔ D for positive f_4 statistics or A ↔ D and/or B ↔ C for negative f_4 statistics. Two-tailed P-values from Z-scores are presented (not corrected for multiple comparisons).

4-population tree: ((A,B);(C,D))	f_4	SE	*Z*-score	Two-tailed
A,B = *C. brontotheroides*, *C. desquamator*				*P*-value
C_brontotheroides,C_desquamator; C_higuey_EasternDominicanRepublic,C_variegatus_Long	-0.00407	0.000866	-4.69585	**2.655E-06**
C_brontotheroides,C_desquamator; C_higuey_EasternDominicanRepublic,C_variegatus_Exumas	-0.00404	0.000946	-4.27719	**1.893E-05**
C_brontotheroides,C_desquamator; C_higuey_EasternDominicanRepublic,C_variegatus_AcklinsCrooked	-0.00328	0.000819	-3.99932	**6.352E-05**
C_brontotheroides,C_desquamator; C_variegatus_SanSalvador_PigeonCreek,C_higuey_EasternDominicanRepublic	0.003349	0.000841	3.97933	**6.911E-05**
C_brontotheroides,C_desquamator; C_variegatus_NewProvidence,C_variegatus_Long	-0.00176	0.000478	-3.6929	**0.0002217**
C_brontotheroides,C_desquamator; C_higuey_EasternDominicanRepublic,C_variegatus_Cat	-0.00331	0.000925	-3.57977	**0.0003439**
C_brontotheroides,C_desquamator; C_higuey_EasternDominicanRepublic,C_variegatus_RumCay	-0.00283	0.00084	-3.37171	**0.000747**
C_brontotheroides,C_desquamator; C_variegatus_NewProvidence,C_variegatus_Exumas	-0.00174	0.000543	-3.20991	**0.0013278**
C_brontotheroides,C_desquamator; C_higuey_EasternDominicanRepublic,C_bondi_WesternDominicanRepublic	-0.0029	0.000971	-2.98646	**0.0028223**
C_brontotheroides,C_desquamator; C_higuey_EasternDominicanRepublic,C_variegatus_Venezuela	-0.00317	0.001102	-2.87644	**0.0040219**
C_brontotheroides,C_desquamator; C_variegatus_Long,C_variegatus_Massachussetts	0.001569	0.000559	2.80579	**0.0050193**
C_brontotheroides,C_desquamator; C_higuey_EasternDominicanRepublic,C_variegatus_NewProvidence	-0.0023	0.000824	-2.79436	**0.0052003**
C_brontotheroides,C_desquamator; C_variegatus_Exumas,C_variegatus_Massachussetts	0.001548	0.000595	2.6013	**0.0092871**
C_brontotheroides,C_desquamator; C_higuey_EasternDominicanRepublic,C_variegatus_Massachussetts	-0.0025	0.000968	-2.58022	**0.0098737**
C_brontotheroides,C_desquamator; C_variegatus_Long,C_variegatus_RumCay	0.001235	0.000496	2.48842	**0.0128312**
C_brontotheroides,C_desquamator; C_variegatus_Exumas,C_variegatus_RumCay	0.001213	0.000565	2.14744	**0.0317583**
C_brontotheroides,C_desquamator; C_variegatus_AcklinsCrooked,C_variegatus_NewProvidence	0.000974	0.000462	2.10699	**0.0351184**
C_brontotheroides,C_desquamator; C_variegatus_AcklinsCrooked,C_variegatus_Long	-0.00079	0.000387	-2.04465	**0.0408894**
C_brontotheroides,C_desquamator; C_variegatus_Long,C_bondi_WesternDominicanRepublic	0.001166	0.000577	2.02099	**0.0432808**
C_brontotheroides,C_desquamator; C_bondi_WesternDominicanRepublic,C_variegatus_Exumas	-0.00114	0.000577	-1.98418	**0.0472358**
C_brontotheroides,C_desquamator; C_variegatus_Cat,C_variegatus_NewProvidence	0.00101	0.000576	1.75377	0.0794699

C_brontotheroides,C_desquamator; C_variegatus_SanSalvador_PigeonCreek,C_variegatus_NewProvidence	0.001047	0.000642	1.6302	0.1030592
C_brontotheroides,C_desquamator; C_variegatus_AcklinsCrooked,C_variegatus_Exumas	-0.00077	0.000509	-1.51123	0.1307299
C_brontotheroides,C_desquamator; C_variegatus_Cat,C_variegatus_Long	-0.00075	0.000521	-1.4486	0.1474493
C_brontotheroides,C_desquamator; C_variegatus_Venezuela,C_variegatus_Exumas	-0.00087	0.000625	-1.39907	0.161792
C_brontotheroides,C_desquamator; C_variegatus_Long,C_variegatus_Venezuela	0.000895	0.000646	1.38659	0.1655668
C_brontotheroides,C_desquamator; C_variegatus_Cat,C_variegatus_Exumas	-0.00073	0.000533	-1.37421	0.1693765
C_brontotheroides,C_desquamator; C_variegatus_AcklinsCrooked,C_variegatus_Massachussetts	0.000779	0.000574	1.3566	0.1749083
C_brontotheroides,C_desquamator; C_variegatus_SanSalvador_PigeonCreek,C_variegatus_Long	-0.00072	0.000555	-1.29216	0.1963017
C_brontotheroides,C_desquamator; C_variegatus_Cat,C_variegatus_Massachussetts	0.000815	0.000648	1.25723	0.2086704
C_brontotheroides,C_desquamator; C_variegatus_SanSalvador_PigeonCreek,C_variegatus_Massachussetts	0.000852	0.00068	1.25299	0.2102093
C_brontotheroides,C_desquamator; C_variegatus_NewProvidence,C_variegatus_Venezuela	-0.00087	0.000732	-1.18638	0.2354723
C_brontotheroides,C_desquamator; C_variegatus_SanSalvador_PigeonCreek,C_variegatus_Exumas	-0.0007	0.000631	-1.10222	0.270366
C_brontotheroides,C_desquamator; C_variegatus_Venezuela,C_variegatus_Massachussetts	0.000674	0.000638	1.05681	0.2905983
C_brontotheroides,C_desquamator; C_variegatus_NewProvidence,C_bondi_WesternDominicanRepublic	-0.0006	0.00058	-1.03049	0.30278
C_brontotheroides,C_desquamator; C_variegatus_NewProvidence,C_variegatus_RumCay	-0.00053	0.000538	-0.98417	0.3250314
C_brontotheroides,C_desquamator; C_variegatus_SanSalvador_PigeonCreek,C_variegatus_RumCay	0.000517	0.000551	0.939247	0.3476039
C_brontotheroides,C_desquamator; C_variegatus_AcklinsCrooked,C_variegatus_RumCay	0.000444	0.000494	0.899694	0.3682831
C_brontotheroides,C_desquamator; C_variegatus_Cat,C_variegatus_RumCay	0.00048	0.000538	0.892052	0.3723651
C_brontotheroides,C_desquamator; C_bondi_WesternDominicanRepublic,C_variegatus_Massachussetts	0.000403	0.000521	0.773381	0.4392969
C_brontotheroides,C_desquamator; C_variegatus_AcklinsCrooked,C_bondi_WesternDominicanRepublic	0.000376	0.000564	0.666199	0.5052839
C_brontotheroides,C_desquamator; C_variegatus_SanSalvador_PigeonCreek,C_bondi_WesternDominicanRepublic	0.000449	0.000701	0.640375	0.5219288
C_brontotheroides,C_desquamator; C_variegatus_Cat,C_bondi_WesternDominicanRepublic	0.000412	0.000647	0.636437	0.5244916
C_brontotheroides,C_desquamator; C_variegatus_RumCay,C_variegatus_Massachussetts	0.000335	0.000663	0.505251	0.6133826
C_brontotheroides,C_desquamator; C_variegatus_Venezuela,C_bondi_WesternDominicanRepublic	0.000271	0.000569	0.475545	0.6343986
C_brontotheroides,C_desquamator; C_variegatus_Venezuela,C_variegatus_RumCay	0.000339	0.000739	0.458599	0.6465222
C_brontotheroides,C_desquamator; C_variegatus_NewProvidence,C_variegatus_Massachussetts	-0.00019	0.000639	-0.30466	0.7606236
C_brontotheroides,C_desquamator; C_variegatus_SanSalvador_PigeonCreek,C_variegatus_Venezuela	0.000178	0.000735	0.242249	0.8085872
C_brontotheroides,C_desquamator; C_variegatus_Cat,C_variegatus_Venezuela	0.000141	0.00077	0.182974	0.8548184
C_brontotheroides,C_desquamator; C_variegatus_AcklinsCrooked,C_variegatus_Venezuela	0.000105	0.000668	0.157348	0.8749706
C_brontotheroides,C_desquamator; C_variegatus_SanSalvador_PigeonCreek,C_variegatus_AcklinsCrooked	7.30E-05	0.000543	0.134279	0.893182
C_brontotheroides,C_desquamator; C_bondi_WesternDominicanRepublic,C_variegatus_RumCay	6.84E-05	0.000661	0.10358	0.9175027
C_brontotheroides,C_desquamator; C_variegatus_Cat,C_variegatus_AcklinsCrooked	3.59E-05	0.000525	0.068343	0.9455124
C_brontotheroides,C_desquamator; C_variegatus_SanSalvador_PigeonCreek,C_variegatus_Cat	3.71E-05	0.000665	0.055726	0.95556
C_brontotheroides,C_desquamator; C_variegatus_Long,C_variegatus_Exumas	2.16E-05	0.000451	0.04785	0.9618355

Appendix S1. Species, lake or coastal population, Caribbean island or coastal population location, source/collector, collection date, and sample size for population genetic analyses.

species	population	island	*n*	source	date
Cyprinodon desquamator	Little Lake	San Salvador	3	CHM	7/2011
Cyprinodon desquamator	Crescent Pond	San Salvador	6	CHM	7/2011
Cyprinodon desquamator	Oyster Pond	San Salvador	3	CHM	7/2011
Cyprinodon desquamator	Great Lake	San Salvador	3	CHM	7/2011
Cyprinodon desquamator	Osprey Lake	San Salvador	4	CHM	7/2011
Cyprinodon brontotheroides	Little Lake	San Salvador	6	CHM	7/2011
Cyprinodon brontotheroides	Crescent Pond	San Salvador	6	CHM	7/2011
Cyprinodon brontotheroides	Oyster Pond	San Salvador	3	CHM	7/2011
Cyprinodon brontotheroides	Osprey Lake	San Salvador	4	CHM	7/2011
Cyprinodon brontotheroides	Moon Rock	San Salvador	1	CHM	7/2011
Cyprinodon brontotheroides	Wild Dilly	San Salvador	4	CHM	7/2011
Cyprinodon variegatus	Little Lake	San Salvador	5	CHM	7/2011
Cyprinodon variegatus	Crescent Pond	San Salvador	4	CHM	7/2011
Cyprinodon variegatus	Oyster Pond	San Salvador	2	CHM	7/2011
Cyprinodon variegatus	Six Pack Pond	San Salvador	1	CHM	7/2011
Cyprinodon variegatus	Mermaid Pond	San Salvador	2	CHM	7/2011
Cyprinodon variegatus	Osprey Lake	San Salvador	2	CHM	7/2011
Cyprinodon variegatus	Reckley Field	San Salvador	2	CHM	7/2011
Cyprinodon variegatus	Clear Pond	San Salvador	2	CHM	7/2011
Cyprinodon variegatus	Pain Pond	San Salvador	1	CHM	7/2011
Cyprinodon variegatus	Wild Dilly	San Salvador	2	CHM	7/2011
Cyprinodon variegatus	Moon Rock	San Salvador	2	CHM	7/2011
Cyprinodon variegatus	Great Lake	San Salvador	3	CHM	7/2011
Cyprinodon variegatus	Pigeon Creek	San Salvador	2	CHM	7/2011
Cyprinodon variegatus	Lake George	Rum Cay	3	CHM	5/2011
Cyprinodon variegatus	Port Nelson	Rum Cay	2	CHM	5/2011
Cyprinodon variegatus	Great Lake	Cat Island	3	CHM	5/2011
Cyprinodon variegatus	Turtle Sound	Crooked Island	3	CHM	5/2011
Cyprinodon variegatus	Snug Corner	Acklins Island	2	CHM	5/2011
Cyprinodon variegatus	Great Lake	Long Island	1	CHM	5/2011
Cyprinodon variegatus	Dean’s pond	Long Island	2	CHM	5/2011
Cyprinodon variegatus	Gray’s pond	Long Island	1	CHM	5/2011
Cyprinodon variegatus	Burnt Ground	Long Island	1	CHM	5/2011
Cyprinodon variegatus	George Town	Exumas	2	B. J. Turner	
Cyprinodon variegatus	Lake Kilarney	New Providence	3	CHM	5/2011
Cyprinodon laciniatus	Lake Cunningham	New Providence	1	CHM	5/2011
Cyprinodon variegatus	Harold’s Pond	New Providence	1	B. J. Turner	
Cyprinodon variegatus		Cuba	1	A. Morales	
Cyprinodon ovinus	Falmouth River	Massachussetts	2	B. J. Turner	
Cyprinodon variegatus	Middleburg	Florida	1	C. Butcher	
Cyprinodon dearborni		Bonaire	1	F. Vermuelen	

Cyprinodon dearborni	Isla Margarita	Venezuela	1	B.J. Turner	
Cyprinodon higuey	Laguna Bavaro	Dominican Republic	1	CHM	5/2011
Cyprinodon nichollsi	Laguna Oviedo	Dominican Republic	1	CHM	5/2011
Cyprinodon bondi	Etang Saumatre	Dominican Republic	2	CHM	5/2011

Fig. S1

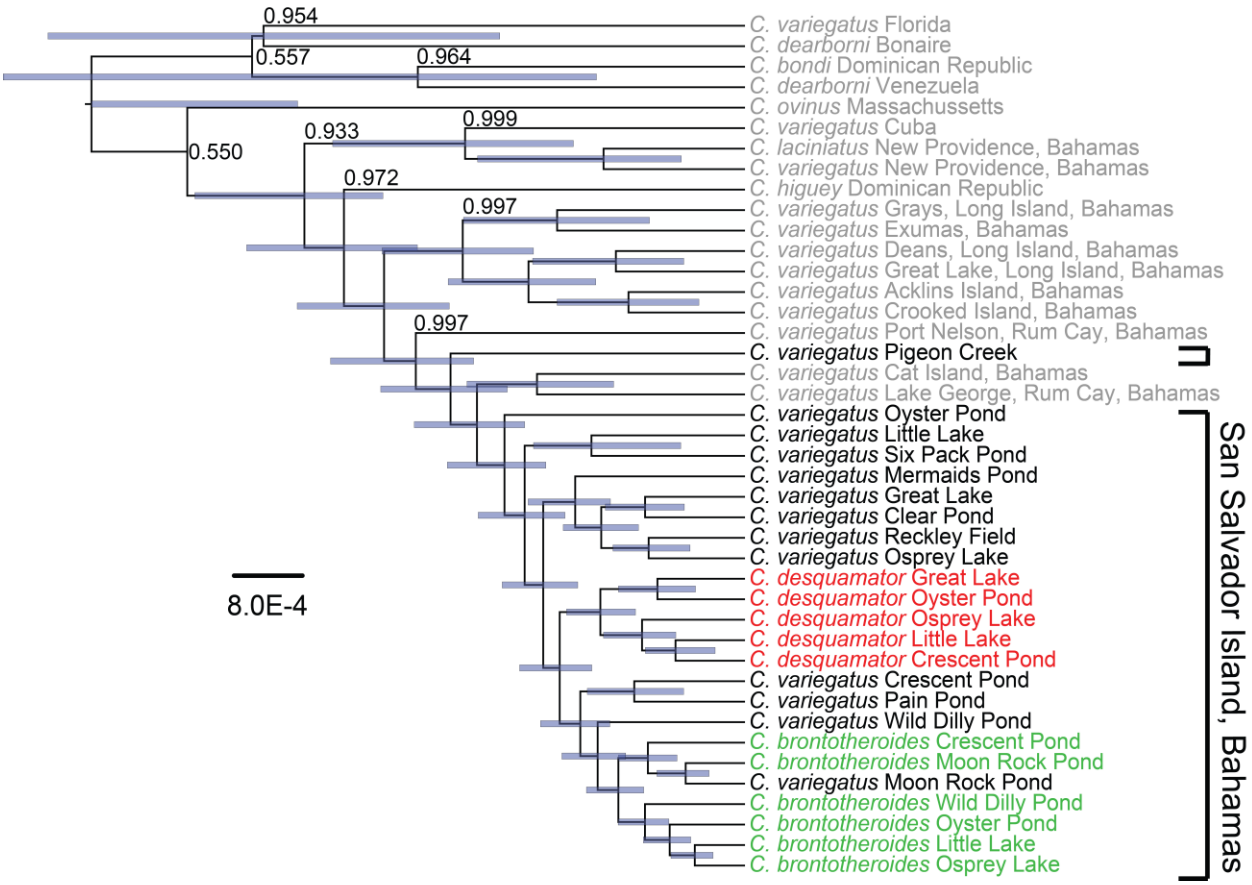

Fig. S1 Time-calibrated *Cyprinodon* phylogeny across the Caribbean estimated from 8,354 concatenated loci using BEAST. Posterior probabilities of each node were equal to 1 unless otherwise indicated.

Fig. S2

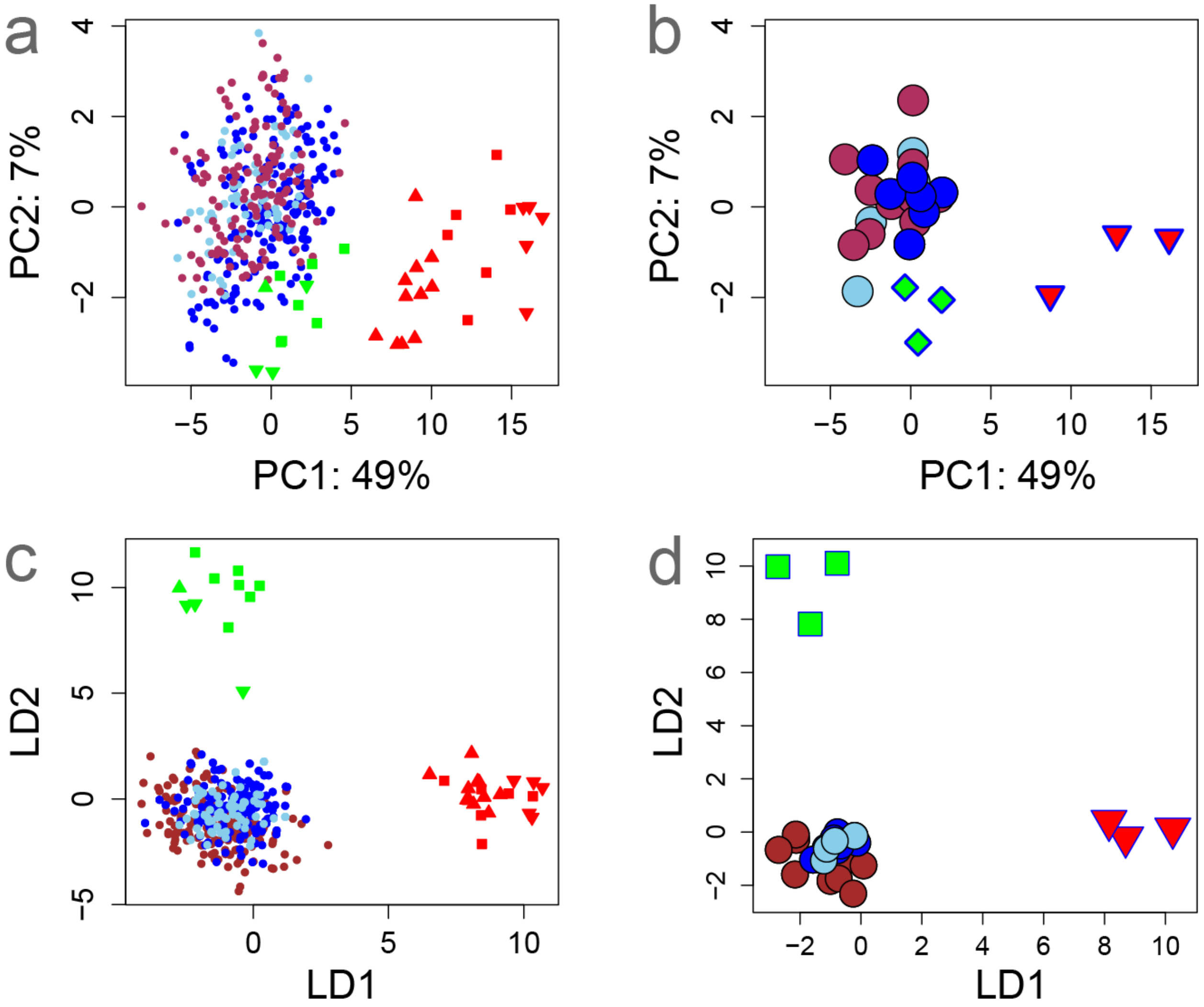

Fig. S2 Morphological diversity for 28 size-corrected skeletal traits in *C. variegatus* generalist populations on San Salvador Island (●generalists on San Salvador sympatric with 1-2 specialist *Cyprinodon* species; ● allopatric generalists on San Salvador); five neighboring Bahamian islands and the Dominican Republic (● allopatric generalist outgroups); three *C. brontotheroides* molluscivore populations on San Salvador (▲▼■); and three *C. desquamator* scale-eating populations on San Salvador (▲▼■). *a-b)* First two principal components of morphological diversity showing *a)* all individuals and *b)* means for each population measured along with percentage of the total phenotypic variance explained by each axis. *c-d)* Discriminant axes maximizing phenotypic separation among the three species showing *c)* all individuals and *d)* means for each population measured. All size-corrected traits were standardized to unit variance before analyses.

Fig. S3

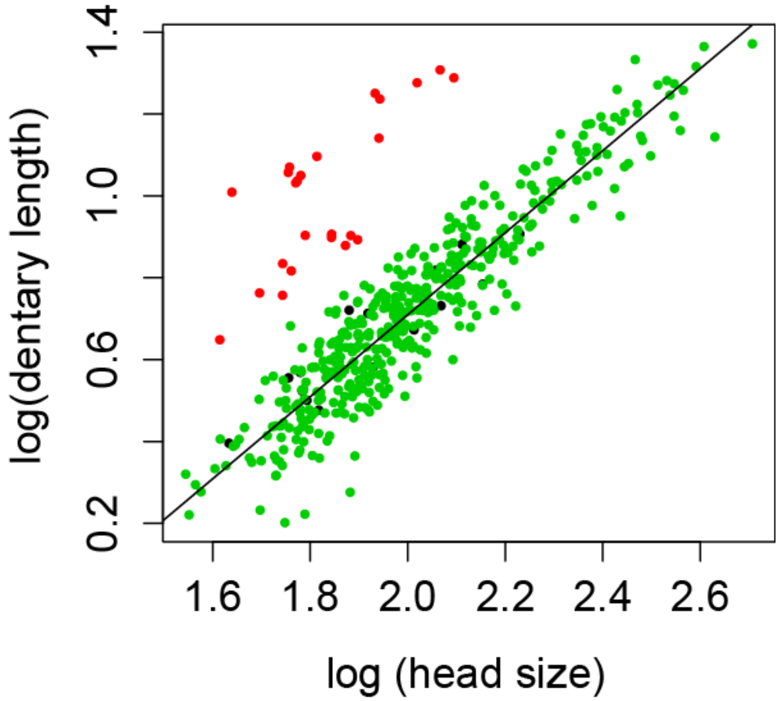

Fig. S3 Lateral photograph of a cleared and stained generalist pupfish specimen illustrating location of all landmarks used for measurement of skeletal traits. Jaws were adducted as shown in all photographs to enable accurate measurement of the quadrate-articular region. Ruler calibration marks are in millimeters; a size standard of 5 millimeters was used to calibrate each image. Photographs were taken with a Canon EOS 60D digital SLR with a 60 mm macro lens. In some cases, damage to skeletal features precluded measurement and only one side was used. Traits were defined by numbered landmarks specifically described in the supplemental methods.

Fig. S4

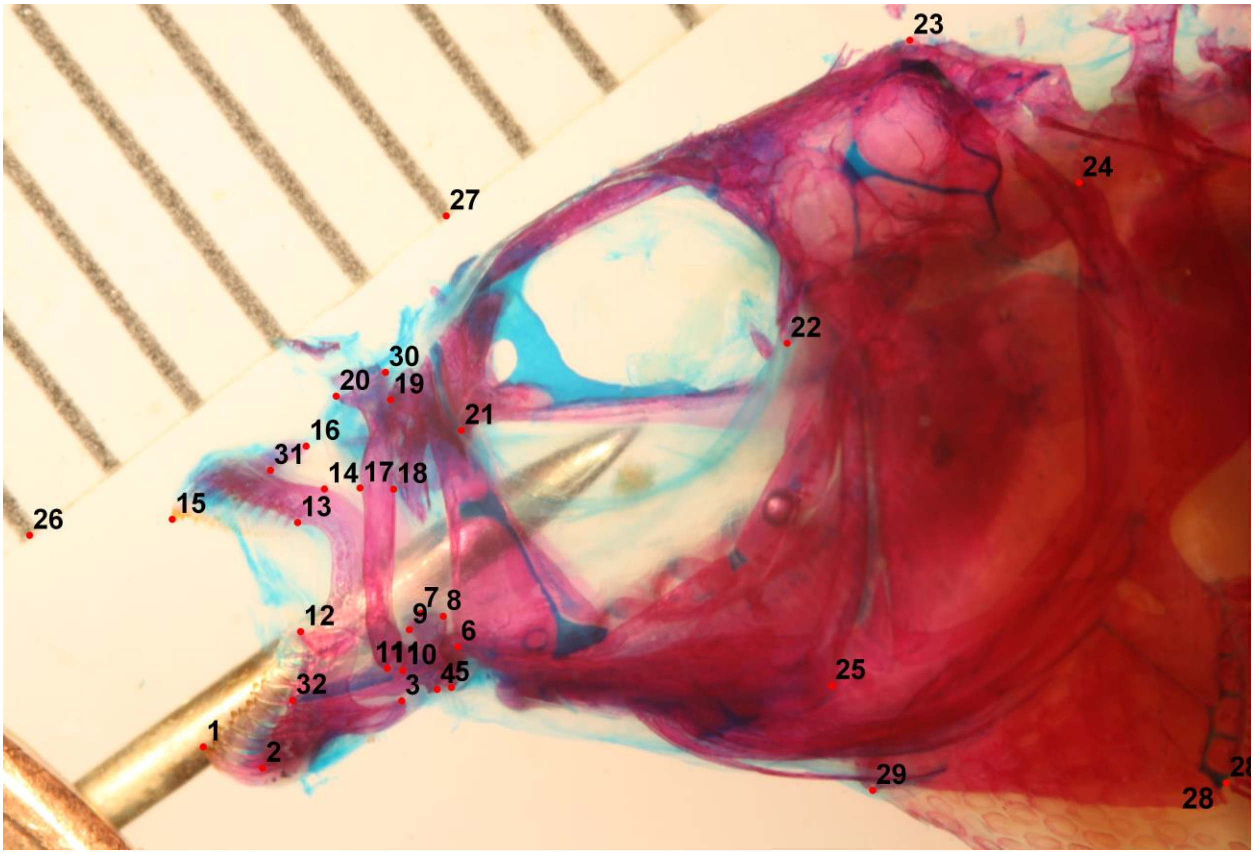

Fig. S4 Representative size-correction plot for dentary length. Log-transformed dentary length relative to log-transformed head size with a linear regression line through all *C. variegatus* individuals (shown in green). All three species (*C. desquamator*: red; *C. brontotheroides*: black; *C. variegatus:* green) exhibit similar allometric scaling coefficients (slopes), but large differences in the intercept and uneven distributions of size among the specimens measured prevented calculation of a single regression line for all individuals. Instead, residual trait values were estimated from a linear regression line through *C. variegatus* individuals only, following (Martin and Wainwright 2013b). Due to an uneven distribution of sizes for each San Salvador species sampled, calculating a linear regression or reduced major axis regression for all three species pooled would not accurately reflect the allometric scaling relationships between trait and overall specimen size. Differences in the y-intercept, but not slope, were observed among the three species for all trait-size linear regressions.

Fig. S5

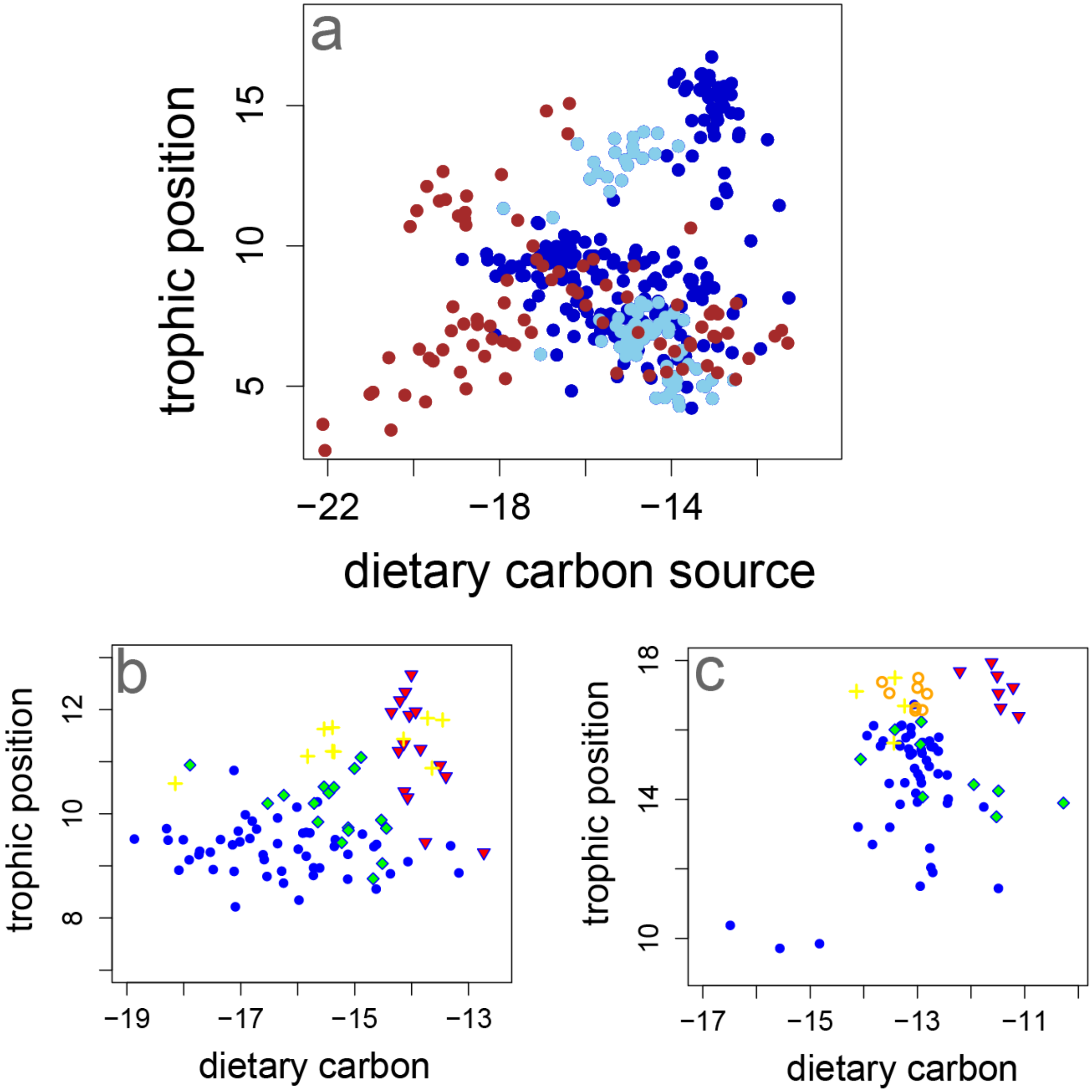

Fig. S5 Individual variation in trophic position (δ15N stable isotope ratio) and dietary carbon source (δ13C stable isotope ratio) across *a)* all *C. variegatus* populations sampled across the Caribbean, *b)* all fish species within Crescent Pond, and *c)* all fish species within Little Lake. ●San Salvador generalist populations from lakes containing specialists, ●San Salvador generalist populations from lakes without specialists, ●generalist populations from neighboring islands.

Panels *b-c* only: ♦molluscivore *C. brontotheroides* individuals, ▼scale-eater *C. desquamator* individuals, + mosquitofish *Gambusia hubbsi*, and ○ silversides *Atherinomorus stipes* within each lake. Only Little Lake contains *A. stipes*. Note different absolute positions along δ15N and δ13C axes for each lake, reflecting different food chain lengths and contributions from four major sources of primary production: terrestrial inputs, phytoplankton, macroalgae, and wigeongrass *Ruppia maritima*.

Supplemental Methods

Sampling

Specimens were immediately sampled for fresh muscle tissue from the caudal peduncle for stable isotope analyses and transferred to 95% ethanol for long-term storage. Muscle tissues were either immediately dried at 60°C or stored with desiccant (magnesium perchlorate) before eventual drying at 60°C for at least twenty-four hours. This desiccant contains no nitrogen or carbon and did not bias isotope ratios in laboratory trials (Martin 2013).

Genomic sequencing and bioinformatics

DNA was extracted from muscle tissue or fin clips of each individual using DNeasy blood and tissue kits (Qiagen, Inc.) and quantified using Picogreen fluorescence and Nanodrop spectrophotometry. The genotyping by sequencing protocol (Elshire et al. 2011) was used as described previously (Martin and Feinstein 2014) using SbfI and NlaIII restriction enzymes without size-selection or streptavidin purification steps. Twelve cycles were used for amplification across two independent reactions per library to limit PCR error. Individuals were individually barcoded using ninety-six 4-8 bp molecular barcodes generated by Deena Bioinformatics (http://www.deenabio.com/services/gbs-adapters) and pooled into two 96-well trays. In addition to the original 96 individuals from San Salvador sequenced for a previous study (Martin and Feinstein 2014), I sequenced an additional 96 individuals from across the Caribbean on one Illumina HiSeq2000 lane at the Vincent J. Coates Sequencing Center, University of California, Berkeley. Paired-end 150-bp reads were obtained from the original sequencing lane and paired-end 100-bp reads were obtained from the second lane. Respectively, 601 million 150-bp and 356 million 100-bp raw reads were sequenced (inclusive of paired ends).

Raw reads were initially assessed for quality using FastQC (Babraham Bioinformatics Institute). Reads were then quality-filtered and demultiplexed using the process_radtags script in the Stacks pipeline (v. 1.23; Catchen *et al.* 2013) with default settings and barcode rescue and then aligned to the *Cyprinodon variegatus* draft genome assembly (v. 1.0, 1035 Mb, 81x coverage, N50 scaffold size = 835 kb) using bowtie2 (Langmead and Salzberg 2012) with very sensitive local alignment settings. Local alignment allows for trimming ends of reads with declining quality scores or chimaeric reads before alignment (Langmead and Salzberg 2012). A total of 651 million reads uniquely aligned to the *Cyprinodon variegatus* assembly.

Aligned reads for each individual were then run through the Stacks pipeline for genotyping (Catchen et al. 2011, 2013). Loci were identified within each individual from a minimum stack size of 3 identical aligned reads (-*m* 3) following recommended guidelines for the Stacks pipeline which generates a large number of identical reads due to filtering by shared restriction enzyme cut sites (Catchen et al. 2011, 2013). PCR error was minimized by reducing cycle number to 12 and running multiple PCR reactions per genomic library (Puritz et al. 2014). Homologous loci across individuals were merged by genomic position (-g) to form a catalog of all loci across individuals. SNPs were called by calculating the likelihood of the two most frequently observed genotypes at each position and performing a standard likelihood ratio test of the homozygous or heterozygous hypotheses using a chi-squared distribution with one degree of freedom (Catchen et al. 2013). Loci with a minimum of read depth of 10 (-*m* 10) were exported from the Stacks pipeline. PLINK (Purcell et al. 2007) was used to further filter the dataset for loci genotyped in >50% of individuals and individuals genotyped at >5% of loci. Additional filtering criteria were applied dependent on the needs of downstream analyses.

Maximum likelihood phylogenetic inference

I also used a traditional concatenation approach to estimate a time-calibrated phylogeny for all *C. variegatus*-complex Caribbean populations, sampling one individual per population. A strict fasta file was exported from Stacks using the population script and filtered for 8,352 loci present in at least 50% of 36 taxa with a minimum of 10 aligned reads. This matrix was then sorted by locus with a custom perl script and concatenated into a single nexus file using Geneious (v. 7.1.7 (Kearse et al. 2012)). A single haplotype was sampled from one high-coverage individual per population. The tree prior was modeled as a coalescent process with constant population size. Nucleotide substitution rates were modeled with a general time-reversible model (GTR) plus gamma-distributed rate variation across loci. I used an uncorrelated lognormal molecular clock with a fixed mean rate of 1, so that branch lengths were estimated in relative time. This avoids some uncertainty in choice of calibration priors for the *Cyprinodon* tree (Martin et al. 2016) and time-calibration to absolute scales is not necessary for this study. There is minimal variation in generation time among *Cyprinodon* species, but substantial changes in ambient temperatures among habitats which may affect mutation rates (Martin et al. 2016). Twelve independent MCMC chains were run on the CIPRES cluster (Miller et al. 2010) using BEAST (v. 1.8.1 (Drummond and Rambaut 2007)) for up to 200 million generations each. Convergence on the stationary distribution required many generations with so much data and most runs did not have sufficient time to converge, as determined using Tracer (v. 1.6). Three out of the twelve runs converged on the stationary distribution after 6 million, 18 million, and 18.5 million generations, respectively. Nine runs did not converge due to an insufficient number of generations (runs were terminated due to maximum allotted CPU hours on the CIPRES cluster). After discarding burn-in, these three runs were combined for a total of 227 million generations. Effective sample sizes exceeded 30 for all parameters in the combined stationary chain. Trees were then sampled systematically every 2000 steps along the combined chain for estimation of the maximum clade credibility tree and posterior probabilities of each node.

Species tree inference

Species tree inference

To estimate the species tree for Caribbean pupfishes, I used SNAPP, which integrates over all sampled gene trees (Bryant et al. 2012). To limit the computational demands of this analysis, I restricted the dataset to 1,534 SNPs genotyped completely in 21 focal Caribbean populations (Appendix S1: *n* = 70 individuals; mean = 3.3 per population) and pooled closely related hypersaline lake populations on Crooked/Acklins Islands, New Providence Island, and Long Island (however, note that complete sampling also introduces bias towards conserved genomic regions). Only 1 SNP was sampled per RAD locus to reduce linkage disequilibrium. Using BEAST2 (v. 2.2.0; Bouckaert et al. 2014) with the SNAPP plug-in (Bryant et al. 2012), two chains were run for 150,000 and 275,000 generations, respectively, and converged after 60,000 and 100,000 generations of burn-in, assessed using Tracer (v. 1.6; Drummond and Rambaut 2007). Due to slow run times on an 8-core Pentium i7 machine (1 million generations every 8,000 hours or 333 days), large effective sample sizes of parameters were not obtainable, which ranged from 3 – 170, affecting several theta parameters. After discarding burn-in, trees were sampled every 100 generations from both runs and visualized using Densitree in BEAST2 (Bouckaert et al. 2014).

Morphometrics

After removing or remeasuring outlier measurements in the dataset, log-transformed linear distances were regressed against log-transformed head size of *C. variegatus* individuals as an index of overall size (Fig. S4). Size-corrected trait residuals were used for surveys of morphological diversity across generalist populations. Residual population mean trait values calculated from a linear regression of population mean log-transformed head size were used for phylogenetic comparative analyses so that each lineage was weighted equally for the size-correction procedure (i.e. some populations had greater sample sizes than others: Appendix 1; see Martin and Wainwright 2011).

Traits were defined by the following numbered landmarks (numbers correspond to numbered traits in Table S1; landmarks correspond to numbered labels in Fig. S2):

Mandibular traits

(1) Lower jaw length (landmarks 1-6) was measured from the center of the jaw joint to the tip of the most anterior tooth on the dentary. (2) Dentary length (landmarks 1-3) was measured from the tip of the most anterior tooth to the posterior tip of the dentary. (3) Jaw opening lever (landmarks 5-6) was measured from the jaw joint to the attachment of the interopercular mandibular ligament on the angular. (4) Jaw closing lever (landmarks 6-7) was measured from the jaw joint to the most distal tip of the articular coronoid process, a proxy for the insertion of the adductor mandibulae on the articular. (5) Coronoid width (landmarks 8-9) was measured as the widest point of the articular coronoid process parallel to the anteroposterior axis. (6) Angular length (landmarks 6-32) was measured from the jaw joint to the distal tip of the internal cartilage of the anterior process of the angular inserted within the dentary. (7) Retroarticular width (landmarks 4-5) was measured from the attachment of the interopercular mandibular ligament on the angular to its articulation with the

retroarticular region. (8) Tooth length (landmarks 1-2) was measured from the root to the tip of the most anterior fully emerged tooth on the dentary.

Premaxillary traits:

(9) Premaxilla width (landmarks 10-12) was measured from the ventral tip of the postmaxillary process to the anterior dorsal tip of the caudal process. (10) Premaxilla length (landmarks 10-15) was measured from the tip of the most anterior tooth on the dentigerous process of the premaxilla to the posterior ventral tip of the postmaxillary process. (11) Upper jaw length (landmarks 6-15) was measured from the jaw joint to the tip of the most anterior tooth on the dentigerous process of the premaxilla. (12) Premaxilla thickness (landmarks 13-14) was measured from the widest point on the lateral ascending arm of the dentigerous process of the premaxilla. (13) Dentigerous process width (landmarks 15-31) was measured from the tip of the most anterior tooth to the base of the ascending process of the premaxilla. (14) Ascending process length (landmarks 31-6) was measured from the base to the most distal tip of the ascending process of the premaxilla.

Maxillary traits:

(15) Maxilla length (landmarks 10-20) was measured from the posterior ventral tip of the postmaxillary process on the premaxilla to the dorsoanterior tip of the maxillary head. (16) Maxilla rotating arm (landmarks 11-19) was measured from the ventral tip of the ascending arm of the maxilla to the cartilaginous pad on the point of articulation with the palatine sulcus on which the maxilla rotates during jaw protrusion. (17) Maxilla thickness (landmarks 17-18) was measured as the widest point of the ascending arm of the maxilla ventral to the articulation with the palatine

sulcus. (18) Maxilla head protrusion (landmarks 20-30) was measured from the posterior tip of the dorsal head of the maxilla to the anterior tip.

Cranial traits:

(19) Orbit diameter (landmarks 21-22) was measured from the posterior edge of the preorbital to the ventral tip of the infraorbital ring. (20) Neurocranium length (landmarks 23-19) was measured from the dorsoposterior edge of the supraoccipital to the cartilaginous pad on the point of articulation between the maxilla and the palatine sulcus. (21) Neurocranium height (landmarks 23-24) was measured from the dorsoposterior edge of the supraoccipital to the posterior process of the cleithrum at its intersection with the postcleithrum.

Suspensorium and pectoral girdle traits:

(22) Palatine length (landmarks 19-6) was measured from the jaw joint to the cartilaginous pad on the point of articulation between the maxilla and the palatine sulcus. (23) Head height (landmarks 23-29) was measured from the dorsoposterior edge of the supraoccipital to the anteroventral edge of the pelvic girdle. (24) Pectoral height (landmarks 24-28) was measured from the posterior process of the cleithrum to the base of the most ventral fin ray on the pectoral girdle. (25) Pectoral length (landmarks 28-29) was measured from the base of the most ventral fin ray on the pectoral girdle to the anteroventral edge of the pelvic girdle. (26) Adductor mandibulae height (landmarks 25-22) was measured from the ventral tip of the infraorbital ring to the posteroventral edge of the preopercle marking the ventral attachment of the adductor mandibulae. (27) Adductor mandibulae length (landmarks 25-6) was measure from the posteroventral edge of the preopercle to the jaw joint. (28) Quadrate length (landmarks 29-6) was measured from the anteroventral edge of the

pelvic girdle to the jaw joint. (29) Head size (landmarks 6-24) was measured from the jaw joint to the posterior process of the cleithrum.

A note on phylogenetic size-correction

Phylogenetic size-correction (Revell 2009) was not used due to the conflation of specimen size with estimates of trait diversification rates when not explicitly accounting for variation in specimen size during size-correction procedures. For example, in previous exploratory analyses for an earlier study (Martin and Wainwright 2011), after phylogenetic size-correction the residuals of tooth length were still strongly negatively correlated with log SL ($r^2 = 0.36$, $P < 0.0001$). In order to completely isolate trait dimensions from the effect of standard length, I used the residuals from a log trait on log SL regression while acknowledging that species sizes may exhibit phylogenetic signal over macroevolutionary timescales and are statistically non-independent. However, on this population-level scale, variation in collected specimen sizes is often much greater than phylogenetic variation in maximum organism sizes among lineages. Failing to completely remove the effects of specimen size poses substantial problems for downstream analyses, such as overestimating the rate of morphological diversification within clades which exhibit greater variation in specimen size (whether due to sampling variation in the size of collected specimens or biological variation in the maximum adult size of different populations). For example, previous analyses of the Chichancanab pupfish radiation, which exhibits substantial variation in adult sizes, estimated nearly five-fold higher rates of morphological diversification for a phylogenetically size-corrected tooth length than the same trait corrected for size using ordinary least squares regression (Martin unpublished data).